Volume No.06, Issue No. 11, November 2017 www.ijarse.com



Analysis and Design of MOS Current Mode Logic Circuits with Active Inductor Load

Kirti Gupta⁻¹, Neeta Pandey²

¹Dept. of Electronics and Communication, Bharati Vidyapeeth's College of Engineering, Delhi, India

ABSTRACT

This paper presents the analysis and design of an improved version of conventional MOS current mode logic (MCML) known as the shunt-peaked MCML style (MCML-SP) is presented. This logic style employs inductors in the load. The analytical formulation of the shunt-peaked MCML inverter employing active inductor is derived. An approach to design shunt-peaked MCML inverter is also developed which is easily extended to realize complex shunt-peaked digital MCML circuits. The performance of the designed circuits is compared with their respective MCML counterparts through simulations using TSMC 0.18 µm CMOS technology parameters. A maximum delay reduction of 29 % is achieved for shunt-peaked MCML circuits. The impact of process variation on the MCML-SP and conventional MCML inverter at different design corners shows similar variations.

Keywords: Active Inductor, High-Speed, Digital Circuits, MCML, Shunt-Peaked

I INTRODUCTION

The tremendous advancements in the VLSI technology has led to the design of high-resolution mixed-signal applications. These applications demands high performance digital circuits to be fabricated with analog circuitry on the same silicon substrate. MOS current mode logic (MCML) style has been widely used to design of digital circuits for mixed-signal applications as they provide an analog friendly environment due to the low switching noise [1-6].

A high speed version of the conventional MCML logic style named as shunt-peaked MCML logic style has been suggested in literature [7, 8]. This logic style is based on the technique of shunt-peaking and involves the use of inductors. A variety of digital circuits based on the shunt-peaked MCML logic style has been suggested [8-10]. However, the detailed analysis and the design of the shunt-peaked MCML circuits are not presented in any of them. In this paper, the design of shunt-peaked MCML circuits through analytical modeling is put forward.

² Dept. of Electronics and Communication Engineering, Delhi Technological University, Delhi, India

Volume No.06, Issue No. 11, November 2017 www.ijarse.com



The paper first presents an overview of the conventional MCML style in section 2. Then, the analysis of the shunt-peaked MOS current mode logic style employing active inductors is presented in section 3. An approach to design shunt-peaked MCML inverter is formulated in section 4 which is extended for shunt-peaked digital circuits. A variety of digital circuits is designed and is compared with the conventional MCML counterparts through simulations using 0.18 µm TSMC CMOS technology parameters in section 5. The impact of process variation at different design corners is also studied. Finally section 6 concludes the paper.

II MOS CURRENT MODE LOGIC (MCML) STYLE

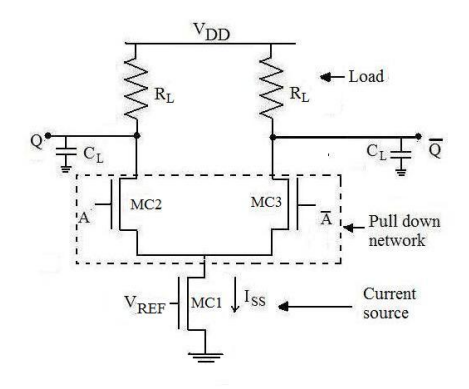
A conventional MCML circuit consists of three main parts: a pull-down network (PDN), a constant current source, and a load circuit. The PDN implements the logic function by applying the series-gating approach [4]. The constant current source MC1 provides the bias current I_{SS} while the load resistor R_L determines the voltage swing. A schematic of a conventional MCML inverter with differential input A is shown in Fig.1. It works on the principle of current steering. When the differential input A is high, the bias current I_{SS} flows through the transistor MC2 and produces a low differential output voltage ($V_{OL} = V_Q - \overline{V_Q} = -I_{ss}R_L$). Conversely, when the differential input A is low, the bias current I_{SS} gets steered to transistor MC3 and produces a high differential output voltage ($V_{OH} = V_Q - \overline{V_Q} = I_{ss}R_L$). Thus, the voltage swing, V_{SWING} defined as the difference in the high and low output voltage is given as:

$$V_{SWING} = V_Q - \overline{V_Q} = 2 I_{SS} R_L \tag{1}$$

The voltage gain A_{v_con} can be computed by applying the half circuit concept [11]. The analysis of Fig. 1b gives A_{v_con} as:

$$A_{v_{-con}} = \frac{v_{Q(s)}}{v_{A(s)}} = \frac{g_{mc 2}R_L}{1 + sR_LC_L}$$
 (2)

where R_L = load resistance, C_L is the load capacitance including the parasitic capacitances of the transistors in the PDN and the interconnect capacitances and g_{mc2} is the transconductance of the transistor MC2.



(a)

Volume No.06, Issue No. 11, November 2017 www.ijarse.com



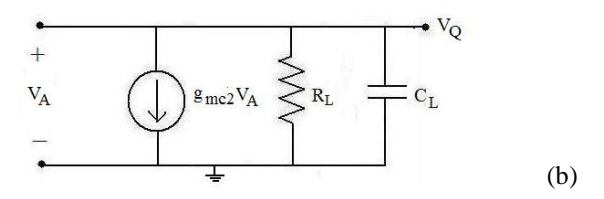


Fig.1. Conventional MCML inverter (a) circuit diagram (b) equivalent half circuit

III SHUNT-PEAKED MCML STYLE

The shunt-peaking technique can be used to increase the speed of the conventional MCML circuits [8]. This technique uses an inductor (L) in series with a resistor (R_{SP}) in the load such that the first-order RC circuit (2) is replaced with a second-order (RLC) circuit. Such circuits are named as shunt-peaked MCML circuits and may be abbreviated as MCML-SP circuits. A schematic of a MCML-SP inverter employing spiral inductor in the load is shown in Fig.2. When the differential input A is high, the bias current I_{SS} flows through the transistor MS2 and produces a low differential output voltage ($V_{OL} = V_Q - \overline{V_Q} = -I_{SS}R_{SP}$) as the inductor L behaves as a short circuit to the constant inputs. Conversely, when the differential input A is low, the bias current I_{SS} is steered to the transistor MS3 and produces a high differential output voltage ($V_{OH} = V_Q - \overline{V_Q} = I_{SS}R_{SP}$). Thus, for the equal values of R_{SP} and R_L , the voltage swing, V_{SWING} of the MCML-SP circuits is same as that of the conventional MCML circuits.

The use of the spiral inductor has several restrictions such as large component size and lengthier design process. Therefore, an active inductor [8] can be used in place of spiral inductor as shown in Fig. 3. The schematic of a MCML-SP inverter employing the active inductor load along with its equivalent half circuit are shown in Fig. 4. The output impedance of the inverter, Z_{out_ac} by neglecting substrate bias effect can be computed from Fig. 4b as:

$$Z_{out_ac} = \frac{s (C_{gs\,4} + C_{gd\,4}) + G_{BIAS}}{s^2 (C_{gd\,4} C_{gs\,4} + C_L C_{gs\,4}) + s [G_{BIAS} (C_L + C_{gs\,4}) + g_{ma\,4} C_{gd\,4}] + g_{ma\,4} G_{BIAS}}$$
(3)

where G_{BIAS} (= 1/ R_{BIAS}) is the conductance in the active inductor, C_L is the load capacitance including the parasitic capacitances of the transistors in the PDN and the interconnect capacitances, and $g_{ma\,4}$, $C_{gs\,4}$, $C_{gd\,4}$ respectively are the transconductance, gate-source capacitance and gate-drain capacitance of the transistor MA4. It can be observed that (7) reduces to $1/g_{ma\,4}$ for the static case.

Volume No.06, Issue No. 11, November 2017 www.ijarse.com



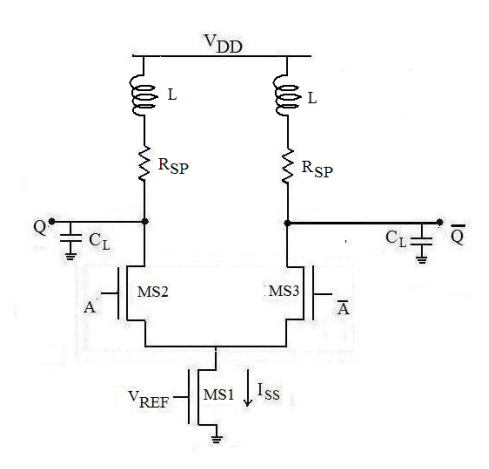


Fig.2. MCML-SP inverter with spiral inductor

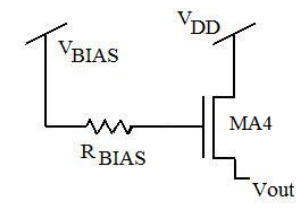


Fig.3. active inductor [8]

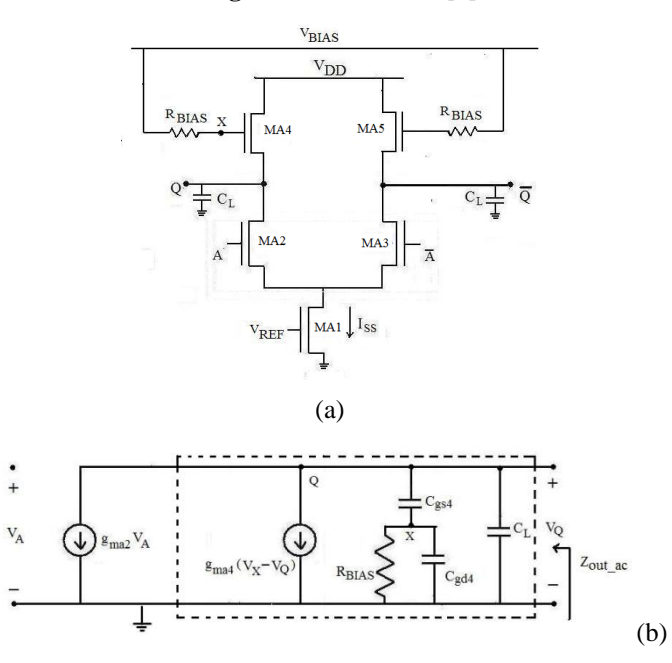


Fig.4. MCML-SP inverter with the active inductor (a) circuit diagram (b) equivalent half circuit

The derivation of the voltage gain A_{v_ac} for the MCML-SP inverter with active inductor load using in the half-circuit concept results in:

Volume No.06, Issue No. 11, November 2017 www.ijarse.com



$$\begin{split} A_{v_ac} \;\; &= \frac{V_Q(s)}{V_A(s)} = \; g_{ma\,2} Z_{out_ac} \\ &= \frac{g_{ma\,2} \big[s \; (C_{gs\,4} + C_{gd\,4}) \; + G_{BIAS} \, \big]}{s^2 (\; C_{gd\,4} C_{gs\,4} + C_L C_{gs\,4} + C_L C_{gd\,4}) \; + \; s \; \big[G_{BIAS} \left(C_L + C_{gs\,4} \right) \; + \; g_{ma\,4} C_{gd\,4} \big] \; + \; g_{ma\,4} G_{BIAS}} \end{split} \tag{4a}$$

where $g_{ma\,2}$ is the transconductance of the transistor MA2,

By assuming $C_{gd4}C_{gs4} \ll C_L(C_{gd4}+C_{gs4})$, the (4a) can be simplified as:

$$A_{v_ac} = \frac{g_{ma} \,_{2} [s \, (C_{gs \,_{4}} + C_{gd \,_{4}}) + G_{BIAS} \,]}{s^{2} C_{L} (C_{gs \,_{4}} + C_{gd \,_{4}}) + s \, [G_{BIAS} \, (C_{L} + C_{gs \,_{4}}) + g_{ma \,_{4}} C_{gd \,_{4}}] + g_{ma \,_{4}} G_{BIAS}}$$

$$(4b)$$

In standard form [12], (4b) can be rewritten as:

$$A_{v_sp}(s) = \frac{(s+z)\omega_n^2/z}{s^2 + 2s\omega_n s + \omega_n^2}$$
(4c)

Comparing (8b) with (8c), the value of the damping factor and natural frequency can be computed as:

damping factor,
$$\varsigma = \frac{1}{2} \left(C_L + C_{gs4} + \frac{g_{ma4}}{G_{BIAS}} C_{gd4} \right) \sqrt{\frac{G_{BIAS}}{(C_{gs4} + C_{gd4})C_L g_{ma4}}}$$
 (5a)

For large values of C_L, (9a) can be approximated as:

damping factor,
$$\varsigma = \frac{1}{2} \sqrt{\frac{C_L G_{BIAS}}{(C_{gs\,4} + C_{gd\,4})g_{ma\,4}}}$$
 (5b)

natural frequency,
$$\omega_n = \sqrt{\frac{g_{ma} \,_4 G_{BIAS}}{(C_{gs} \,_4 + C_{gd} \,_4)C_L}}$$
 (5c)

Depending on the value of the damping factor, ς , the circuit can be overdamped ($\varsigma > 1$), critically damped ($\varsigma = 1$) and underdamped ($\varsigma < 1$) and accordingly the time responses for the three cases differ. The presence of a LHP s-plane zero in (4a) further tends to enhance the speed of the MCML-SP inverter in comparison to conventional MCML inverter.

IV DESIGN OF MCML-SP CIRCUITS

In this section, an approach to size the transistors of the MCML-SP circuits for a given value of bias current, voltage gain and voltage swing is outlined. Firstly, the design method for MCML-SP inverter with active inductor load is discussed. Then, the approach to design MCML-SP digital circuits is developed.

Volume No.06, Issue No. 11, November 2017 www.ijarse.com



4.1 Design of MCML-SP inverter with active inductor load

For the active inductor MCML-SP inverter (Fig. 4), the output impedance derived in (3) reduces to $1/g_{ma\,4}$ for the static case. By solving (1) and then equating to the impedance in the static case, the value of aspect ratio of the load transistors MA4 and MA5 for the given values of the bias current I_{SS} and the voltage swing V_{SWING} , can be calculated as

$$\left(\frac{W_{N}}{L_{N}}\right)_{MA.4.5} = \frac{2 I_{SS}}{V_{SWING} \mu_{eff.n} C_{ox} (V_{DD} - V_{T.n})}$$

$$(6)$$

where the parameters $\mu_{eff,n}$, $V_{T,n}$, W_N and L_N are the effective electron mobility, the threshold voltage, the effective channel width and effective channel length of the load transistors MA4 and MA5 respectively. After determining the size of MA4 and MA5, the different capacitance values are computed. The gate-source capacitance C_{gs} is equal to the overlap capacitance between the gate and the source [4]. The gate-drain capacitance C_{gd} is evaluated as the sum of the overlap capacitance and the intrinsic contribution associated with its channel charge [4].

For a specific value of damping factor, ς and load capacitance C_L , the value of the G_{BIAS} can be computed by using (5b) as:

$$G_{BIAS} = 4 \varsigma^2 \frac{(c_{gs\,4} + c_{gd\,4})g_{ma\,4}}{c_I} \tag{7}$$

The aspect ratio of the transistors MA2 and MA3 in the PDN can be calculated by solving(3) for the static case.

$$\left(\frac{W_{N}}{L_{N}}\right)_{M\Delta 2,3} = A_{V_{-}ac}^{2} \left(\frac{W_{N}}{L_{N}}\right)_{M\Delta 4,5} \tag{8}$$

4.2 MCML-SP digital circuit design

The design approach presented in section 4.2 for MCML-SP inverter design with active inductor loads can be extended to design other MCML-SP circuits. The steps to design the load for the active inductor load remain same as explained in section 4.2.To design the PDN, firstly the size of the equivalent inverter is found out by using either (12) or (15) depending upon the load and then individual transistors are sized according to the conventional approach for MCML circuits as discussed in [4].

V SIMULATION RESULTS

This section first verifies the theoretical propositions presented in section 3 and 4. Thereafter, the performance of different logic gates based on MCML-SP style is compared with the conventional MCML style. The effect of parameter variations is also studied at different design corners. All the simulations are

Volume No.06, Issue No. 11, November 2017 www.ijarse.com



performed by using TSMC 0.18 μm CMOS technology parameters with a power supply of 1.8 V, bias current of 500 μA , voltage swing of 400 mV, and load capacitance of 400 fF.

5.1 Proposed MCML-SP Inverter

The methodology given in Section 3 and 4 is used to design active inductor load inverter with the outlined specifications for different damping factors. The simulations were performed to select the value of damping factor to achieve proper circuit operation and lowest propagation delay. The propagation delay for active inductor load inverter various values of damping factor, are listed in Tab. 1. It can be observed from the table that the propagation delay for the underdamped case is lower than the overdamped and the critically damped cases. For proper operation of the circuit, the overshoot should be less than 5% in the time response [12]. Keeping this in view, the case with $\varsigma = 0.7$ gives the lowest propagation delay. Therefore, this value can be chosen as the optimum value to design MCML-SP circuits. The sizes of the transistors for the active inverter for $\varsigma = 0.7$ are listed in Tab. 2. All the transistors have minimum channel length.

5.2 Performance Comparison

Several logic circuits such as AND/NAND, MUX, full adder, D-latch are designed with active inductor using the method outlined in section 4. The performance of these circuits is compared with their conventional resistive and PMOS [4], spiral inductor load MCML counterparts. It may be noted that all the circuits operate at same supply voltage and bias current therefore they all consume same static power computed as the product of the supply voltage and bias current [4]. The propagation delay of the gate with respect to the above loads is listed in Tab. 3. It can be noted that a delay reduction varying from 21% to 29% is obtained by using inductive load.

The impact of parameter variation on the MCML-SP inverters and the conventional inverters is studied at different design corners. The findings for various operating conditions are given in Tab. 4. It is found that the propagation delay varies by a factor of 1.04, 1.15, 1.11 and 1.10 for the resistive, PMOS, spiral inductor and active inductor load respectively between the best and the worst cases. It can be observed that they all show similar variations.

Table. 1. : Propagation delay of the MCML-SP inverter with active inductor loads for various values of damping factor, ς

Damping factor, ς	Propagation delay with active inductor (ps)	Output response	
2	120	Flat	
1	111		
0.9	108	Overshoots (< 5%)	
0.8	104		
0.7	102		

Volume No.06, Issue No. 11, November 2017 www.ijarse.com

0.1

0.6	99	Overshoots (> 5%)
0.5	95	
0.4	90	
0.3	88	
0.2	85	

Table. 2. Values of the components for the MCML-SP inverter for $\varsigma = 0.7$

84

MCML-SP inverter with active inductor load (Fig. 4a)			
Component	Value		
MA1	$W/L = 5.2 \ \mu m/0.18 \ \mu m$		
MA2, MA3	$W/L = 17.5 \mu m/0.18 \mu m$		
MA4, MA5	$W/L = 8.65 \mu m/0.18 \mu m$		
R _{BIAS}	7.34 ΚΩ		

Table. 3. Comparison in Propagation delay (ps) of MCML logic circuits using different type of loads

Circuit	Type of load	Resistor	PMOS	Spiral Inductor	Active Inductor
Inverter					
AND/NAND		137	158	111	125
2:1 MUX		175	193	149	159
Full	Sum	327	367	289	301
Adder	Carry	332	381	290	322
D-Latch		195	225	161	171

Table 4. Impact of parameter variations on propagation delay (ps) for different inverters

NMOS	T	F	S	F	S
PMOS	T	F	S	S	F
Topology					
Inverter with resistive load	127	125	130	129	128
Inverter with PMOS load	150	140	161	142	158
Inverter with spiral inductor load	100	95	106	105	104
Inverter with active inductor load	115	108	119	117	118

ISSN: 2319-8354

Volume No.06, Issue No. 11, November 2017 www.ijarse.com



6 CONCLUSION

The analysis and design of shunt-peaked MCML style for digital circuit design is presented in this paper. The logic style uses the shunt-peaking technique and suggests the use of inductors in the load. The design method is illustrated for shunt-peaked MCML inverter with the spiral and active inductors. The effectiveness of the shunt-peaked MCML style is demonstrated by simulating different logic gates. It is found that the shunt-peaked MCML circuits are faster than the other MCML variants. The study of impact of process variation at different design corners shows that conventional MCML and MCML-SP inverters show similar variations.

REFERENCES

- [1] Musicer J. M., Rabaey, J. MOS Current Mode Logic for Low Power, Low Noise, CORDIC Computation in Mixed-Signal Environments. In Proc. International Symposium of Low Power Electronics and Design, 2000, 102-107.
- [2] Hassan, H., Anis, M., Elmasry, M. MOS Current Mode Circuits: Analysis, Design, and Variability. IEEE Transactions on Very Large Scale Integration (VLSI) Systems, 13(8),2005, 885 898.
- [3] Nonis, R., Palumbo, E., Palestri, P., and Selmi, L. A Design Methodology for MOS Current-Mode Logic Frequency Dividers, IEEE Transactions on Circuits and Systems— II: Regular Papers, 54(2), 2007, 245-254.
- [4] Alioto, M., Palumbo, G. Model and Design of Bipolar and MOS Current-Mode logic (CML, ECL and SCL Digital Circuits), Springer, 2005.
- [5] Caruso, G. Power-aware design of MCML logarithmic adders. Proc. International Conference on Signals and Electronic Systems, 2010, 281-283.
- [6] Yassmeen, M., El-Hariry, Madian, A. H. MOS Current Mode Logic Realization of Digital Arithmetic circuits. Proc. IEEE International Conference on Microelectronics, 2010, 1-4.
- [7] Worapishet, A., Thamsirinumt, M. An NMOS Inductive Loading Technique for Extended Operating Frequency CMOS Ring Oscillators, Proc. Mid-west Symposium on Circuits and Systems, 2002, 116-119.
- [8] Bui, H. T., Savari, Y. Shunt-Peaking of MCML Gates Using Active Inductors. Proc. IEEE Northeast Workshop on Circuits and Systems, 2004, 361-364.
- [9] Gupta, K., Pandey, N, Gupta, M. A Novel Active Shunt-Peaked MCML-based High Speed Four-Bit Ripple-Carry Adder. Proc. the IEEE International Conference on Computer and Communication Technology, Allahabad (India), 2010, p:285-289.

Volume No.06, Issue No. 11, November 2017 www.ijarse.com



- [10] Gupta, K., Pandey, N, Gupta, M. Shunt-Peaking in MCML Memory Element Design in 0.18μm CMOS Technology.Proc. IEEE INDICON, Kolkata (India),2010, 1-4.
- [11] Razavi, B. Design of Analog CMOS Integrated Circuits, Mc-Graw Hill Higher Education, 2001
- [12] Nagrath I. J., Gopal, M. Control System Engineering, New Age International Publishers, 2006.
- [13] Yuan, F. CMOS Active Inductors and Transformers, Springer 2007.